



Research Journal of Pharmaceutical, Biological and Chemical Sciences

NaCl – Activated Jordanian Bentonite for Olive Mill Waste water Treatment: Evaluation of Physicochemical Properties, Adsorption of Phenolic Compounds: Isotherms and Thermodynamic Studies.

Khansaa Al-Essa*.

Department of Chemistry, University of Jerash, Jerash 26150, Jordan

ABSTRACT

Jordanian bentonite shows a small amount of efficiency in the treatment of OMWW. It is for this reason that NaCl activation of bentonite is undertaken, in order to promote its adsorptive capacity. This work aims to characterize the activated bentonite (AJB) using FTIR, XRD, TGA and BET surface area. It is found that the structural cations have been released from the octahedral positions, thereby exchanging with Na⁺ ions. Differences of surface area were noticed from (66.2 to 249.6m²g⁻¹), which is caused by structural changes of bentonite. The efficiency of AJB towards OMWW treatment was investigated. Batch and column techniques were applied. Physicochemical parameters of OMWW were measured before and after treatment. The adsorption of total phenolic compounds onto AJB was examined with respect to the adsorbent dosage, initial concentration and temperature. The Langmuir and Freundlich models were applied to describe equilibrium isotherms and both models fitted well. The maximum adsorption q_m was found as 8.81 mg/g at 323K. Thermodynamic parameters, free energy (ΔG°), enthalpy (ΔH°) and entropy (ΔS°) of adsorption were also calculated. These parameters show that the adsorption process was feasible, spontaneous and endothermic in nature. Furthermore, the percentage removal of Zn, Fe and Mn ions were also tested and the results show that AJB totally removed all heavy ions, regardless of their initial concentrations. Thus, the cost-effective and easily activated bentonite has a wide potential as an adsorbent and could be very helpful to monitoring the environmental impact of OMWW.

Keywords: Sodium activated bentonite, Low cost adsorbent, Olive mill wastewater, Adsorption isotherms

**Corresponding author*



INTRODUCTION

The demand for olive oil is rapidly increasing worldwide. Mediterranean region producer countries have been facing a serious challenge to find an environmental and economic solution for the disposal and reuse of olive mill wastewater (OMWW). OMWW, the liquid by-product generated during olive oil extraction, is characterized by extremely high concentrations of organic matter and phenols and very low pH values [1]. Moreover, it has high chemical oxygen demand (COD), biological oxygen demand (BOD), solid matter [2] and suspended solids [3]. Direct discharge of OMWW into the environment is forbidden by law. However, disposal of OMWW into the soil affects its quality and harms plant life [4]. In addition, it is a genuine threat to surface and ground water [5]. In Jordan, OMWW is mostly generated from small mills that have limited financial resources and they are usually a great distance from each other. The latter creates difficulty in establishing a central treatment location with and disposal facilities. Among these practices, recycling and the reuse of processed water for irrigation and industrial purposes may be considered. In addition, in order to avoid expensive OMWW treatment investments, the application of economical treatment methods is required. Such methods should be safe for the environment, without harming the small producers in the olive oil industry. Adsorption is an efficient and economical process. The efficiency of this technique depends on the nature of the adsorbent [6]. Adsorbents, such as clay has been used to treat wastewater. Bentonite clay (hydrated aluminum silicate) is the most preferable clay for the removal of different contaminants from wastewater [7]. However, several researchers have proposed the use of bentonite as an adsorbent for removing organic [8,9], anionic and cationic pollutants [10,11], in addition to inorganic pollutants, such as heavy metal ions [12-15].

The adsorption of pollutants, especially heavy metal ions, through the use of bentonite has been studied extensively over the past decade [12,13,14]. Moreover, bentonite has been activated in order to enhance its adsorption capacity, such as acid activation [15,16], organo activation [17,18], nano-bentonite composite [19,20], polymer-bentonite composite [21,22] and other methods [23,24]. However, there are still few references that focus on OMWW treatment using low cost modified bentonite [25] and therefore an adsorption isotherms study of total phenolic compounds removal, including the effect of different parameters on adsorption efficiency, needs to be undertaken.

In Jordan, there are good reserves of bentonite. Jordanian Bentonite has distinguished physical and chemical properties, such as hydrophilicity, biocompatibility, biodegradability and non-toxicity properties. However, its most unique property is its adsorption, due to its high specific surface area and cation exchange capacity (53-85 Meq/100g) [26]. Some researchers have studied the adsorption capacity of this bentonite for Pb(II) [27], Th(IV), U(VI) [28] and Co(II), Ni(II) [29]. However, the activation of this bentonite and its adsorption capacity toward pollutants in OMWW has not been studied in detail.

The objectives of this work are to: (1) characterize the OMWW that comes from different, olive oil mills in Jordan; (2) study the activation of Jordanian Ca-bentonite by sodium chloride; (3) explore the activated Jordanian bentonite (AJB) as an adsorbent for the removal of heavy metal ions, such as Zn, Fe and Mn ions and total phenolic compounds from OMWW; (3) discuss the effect of the adsorbent dosage, the initial concentration and temperature on adsorption efficiency; (4) determine the adsorption isotherms and simulate the experimental data with the Langmuir and Freundlich adsorption models; and (5) investigate the thermodynamic parameters of the total phenolic compounds adsorption onto AJB adsorbent.

MATERIALS AND METHODS

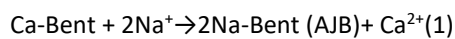
Adsorbent: Purification, Activation and Characterization

The natural Jordanian bentonite clay used in this study was collected from the airport region, Al Azraq. The sample was crushed to particle size $>250\mu\text{m}$ using a ball mill instrument and clay fractions were

obtained by wet sedimentation. The sample was purified in a laboratory, in order to remove quartz, carbonates, calcites, iron hydroxide and organic metals. It was dispersed in distilled water at 22°C and the clay fraction was recovered by centrifugation. This process was repeated four times for each sample, in order to guarantee obtaining samples in a pure form. The samples were dried in an oven at 60°C, then ground and sieved using a 63µm mesh, and stored in tightly closed plastic bottles for use in the experiments.

The purified bentonite (PB) was prepared for sodium activation: 17g ± 0.01g of the purified sample was weighed into a flask and 250mL of 1.0 M NaCl was added. The resulting suspension was stirred at room temperature for 48 hrs. At the end of the mixing duration, the resulting slurry was poured into a Buchner funnel. The residual bentonite was washed with deionized water several times, until it was released from Cl⁻¹ ions against 5% AgNO₃ solution. After drying the sample at 70°C for 24 hours, it was re-ground to reach 300µm particles size and stored in tightly closed plastic bottles to be used in adsorption studies.

The following reaction had occurred:



PB and AJB were characterized by FTIR spectroscopy (Thermo Nicolet NEXUS 670 Spectrophotometer), XRD (Philips X pert pro) and TGA (NETZCH STA 409 PG/PC Thermal Analyzer). BET surface area analysis was determined using Gemini VII from micro meritics.

OMWW: Collection, pretreatment and Characterization

OMWW was obtained from three different olive oil mills located at Jerash city, considering centrifuge processing. Samples were kept refrigerated at -2°C in tightly closed plastic containers. As a pre-treatment, aliquots of 1L of OMWW were centrifuged at 10,000 rpm for 30 minutes and double simple filtration was undertaken, in order to obtain a clear and dark (brownish) solution.

Fresh OMWW was fully characterized before and after treatment. pH, electrical conductivity (EC), DO, ORP, TDS and salt were measured using a Crison PL-700AL meter. COD, alkalinity, total nitrate, total phosphate and total chlorine concentrations were determined using a COD and multi parameter bench meter, PN HI83099-02.

The total phenolic compounds were evaluated by spectrophotometry using the Folin-Ciocalteu method. Briefly, a 2.5mL portion of Folin-Ciocalteu reagent 0.2N was mixed with 0.5mL of the sample. The reaction was kept in the dark for five minutes. Then, 2mL of a sodium carbonate solution (75 g/L) was added to the mixture and the reaction was kept in the dark for one hour. The absorbance was measured at 765 nm in AAS. Contents of the total phenolic compounds in OMWW were expressed as Gallic acid equivalents in grams per litre (g GAE/L residue) [30]. K⁺ and Na⁺ concentrations were determined using a flame photometer (Corning 400). For the heavy metal ions determination tests, Zn, Fe and Mn, a standard solution of each metal ion concentration was prepared in NaClO₄ at pH= 6. The pH of these solutions was adjusted using 0.1 M HCl and 0.1 M NaOH, in order to achieve the desired values. Concentrations of the metal ions were determined using a Varian Spectra AA-250 pulse atomic adsorption spectrometer (AAS).

Adsorption Experiments

The adsorption experiments were carried out by a batch technique. The effect of solution temperature, the mass of AJB and the initial concentration of total phenolic compounds on the percentage removal were studied. Moreover, the AJB was tested for the adsorption of heavy metal ions from OMWW using a column technique. Adsorption processes were carried out in a column of 560mm length, and 12mm

diameter. 1.00 g ± 0.0001 g of adsorbent were packed in a column and 100mL of OMWW was passed through the column. The flow rate was of 1 mL/12min) and the effluent was collected as 10 separate samples, each having a volume of 10 mL. Finally, all analytical experiments were applied at least in duplicate and the mean values are presented in Figs. 4 to 13.

Concentration of adsorbate retained in the adsorbent phase (q, mg g⁻¹) was calculated from the following equation:

$$q = \frac{(C_i - C_e)}{m} * V \quad (2)$$

Where q is the adsorbent phase concentration after equilibrium (mg adsorbate/g adsorbent); C_i and C_e are the initial and final (equilibrium) concentrations of adsorbate in solution (mg/L); V is the solution volume (L); and m is the adsorbent mass (g). Percentage (%) removal of adsorbate was calculated using the following equation:

$$\% \text{Removal} = \frac{(C_i - C_e)}{C_i} * 100 \quad (3)$$

RESULTS AND DISCUSSION

Characterization of adsorbent

FTIR spectra

The FTIR analysis of the RB and AJB were utilized, in order to determine the functional groups on the surface of bentonite responsible for adsorption and to explore the effect of sodium activation on its chemical composition, which is shown in Fig.1.

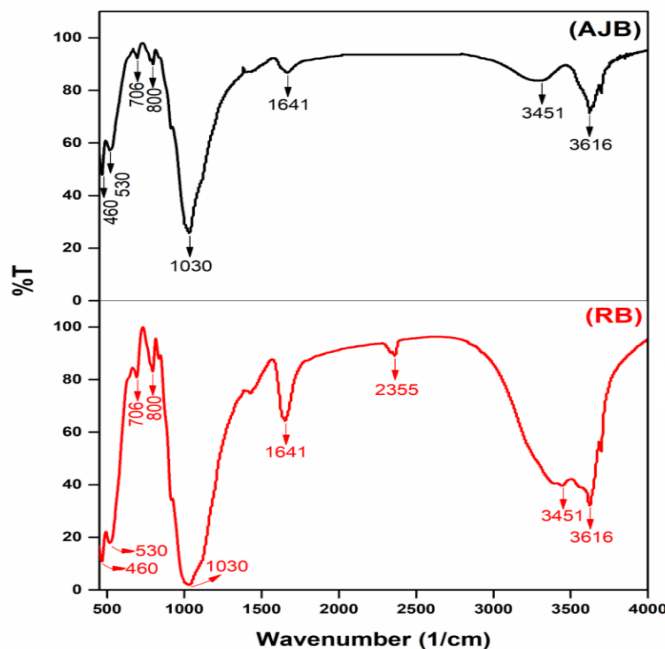


Fig 1: FTIR spectra of RB and AJB.

From RB spectrum, absorption bands resulting from bending vibrations of Si–O groups are found in the 550–400 cm^{-1} region. The bands due to Si–O–Al and Si–O–Si deformations in the spectra occur near 530 and 460 cm^{-1} , respectively [31]. The spectrum also contains a band at 706, 800 and 2355 cm^{-1} which is all attributed to quartz [32,33]. A broad complex band near 1030 cm^{-1} is related to stretching vibrations of Si–O groups [34]. On the other hand, the peak at 1641 cm^{-1} is for H–O–H bending and the stretching vibration of OH appears at around 3451 cm^{-1} . The adsorption band at 3616 cm^{-1} in the spectrum is assigned to stretching vibrations of the structural OH groups of dioctahedral bentonite.

After sodium activation, the most significant change was a decrease in the intensity of the band of the Si–O stretching region at 1030 cm^{-1} . This means that upon the activation process, there is a possibility of the formation of three-dimensional networks of amorphous silica, which may expose more adsorption sites. The increased amount of amorphous silica, as sodium activation progresses, resulted in deterioration of the tetrahedral layer. The intensity of bending and stretching bands characterized the octahedral sheet for Al–Al–OH at a 1641 cm^{-1} decrease, which indicates destruction of the octahedral layer. Moreover, a sharp decrease in the absorption band attributed to the OH vibration at 3616 cm^{-1} is due to the removal of the octahedral cations, thus causing the loss of water and hydroxyl groups coordinated to them [35]. This might indicate the presence of free OH sites on activated bentonite. The decrease in the characteristic band of bentonite appears at 3451 cm^{-1} “which represents the fundamental stretching vibrations of different –OH groups present in Mg–OH–Al, Al–OH–Al, and Fe–OH–Al units in the octahedral layer” [36] and this refers to deterioration of this layer. Furthermore, in regard to quartz bands, the disappearance of the band at 2355 cm^{-1} is noted and also a decrease in the intensities of bands at 706, 800 cm^{-1} , which offers a strong indication that the activation process improves the purity of the bentonite.

Finally, following the activation process, most band positions did not change, thus suggesting that the basic bentonite structure did not collapse.

X-ray diffractograms

The X-ray diffraction patterns of RB and AJB samples are illustrated in Fig. 2. Patterns of RB montmorillonite were the main mineral. However, minor amounts of kaolinite, quartz, gypsum and cristobalite were also identified [37].

As seen from the AJB patterns, the XRD results indicate that changes in the structure of the RB are induced by adding NaCl. The peaks of quartz are diminished and no quartz was present in the AJB sample. The main montmorillonite peaks are present. Two distinct diffraction lines belonging to crystalline NaCl (35 and 55 Å) are seen, thus proving the accumulation of crystalline NaCl [38]. X-ray results of activated bentonite show there is a shift in the position of a few peaks (for example, 31.2 to 26.6 Å). Actually, after the addition of NaCl, the Na^+ ions are absorbed to the surface of the montmorillonite crystal grains to form a hydrated shell [39]. This is an indication of dissolution of the tetrahedral and octahedral sheets and subsequent release of the structural cations: that is, these cations have been eliminated from the octahedral positions, thereby exchanging with Na^+ ions. Moreover, the interlamellar spacing between crystal grains is compressed [40]. The influence of chemical composition and inner structure on the behavior of AJB is obvious. Distinctly, XRD analysis provides good evidence that the adsorptive power of AJB has increased.

Clearly, the activation process causes a decrease in peak intensity. This mostly occurs in the case of montmorillonite, which means a reduction in its content. Also, the quartz content, which is seen as an impurity, disappears after activation. Furthermore, the peaks of RB patterns have relative symmetry, but the peaks of AJB patterns are moving to more dissymmetry. In addition, the appearance of splitting in some peaks, which is an indication of phase transformation to a lower symmetry or partial distortion of its structure, indicates that small distortions can often be observed with peak broadening. These characteristics apparently indicate that bentonite is well activated by Na^+ ions.

The reduction in intensity and increase in the width of peaks at 24.1 Å indicate that the crystallinity of the bentonite is considerably affected by the activation and thus the bentonite crystalline structure is decomposing, which means that the activation process is accompanied by the appearance of an amorphous phase, as confirmed by IR results.

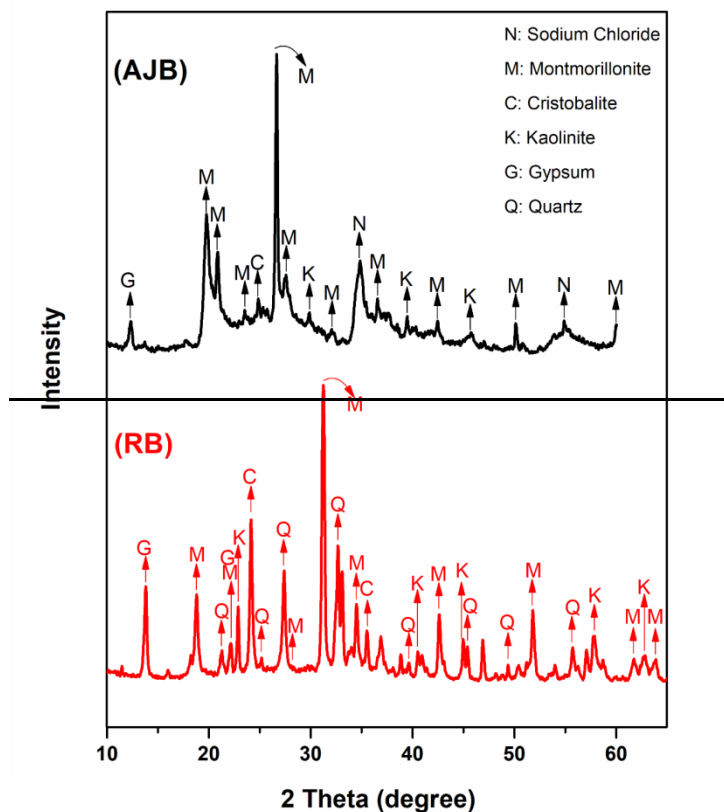


Fig 2: X-ray diffraction patterns of the RB and AJB.

Thermogravimetric analysis (TGA)

Thermogravimetric analysis was undertaken in order to investigate the effect of activation of bentonite with NaCl. Fig. 3 shows a distinct endotherm with a maximum between 30°C and 200°C that corresponds to the release of physically adsorbed water and the dehydration process. Dehydroxylation was executed with more and more favorable temperature, moving from 325 to 720°C. Decomposition of chemically bound water (OH⁻) is detected by an endothermic change with a maximum at 350°C. The dissociation of accumulated NaCl crystals is confirmed at 800°C [41]. The total mass losses within the temperature interval 30–200°C of RB is much more than ABJ. Beyond this temperature, there are higher mass losses for AJB and this is attributed to the dissociation of crystalline NaCl at 800°C. This finding confirms those of the XRD results that show partial deterioration of the AJB microstructure.

The results obtained confirm the formation of NaCl crystals in the AJB, where the accumulated NaCl crystals have a destructive effect mainly on the bentonite microstructure: and as a secondary effect on its increase in permeability. This is enhancing its adsorption capacity toward heavy metal ions, phenolic compounds and other pollutants.

Furthermore, the TGA result is in clear agreement with the FTIR and XRD studies, which indicate consecutive changes of the bentonite sheet upon the activation process.

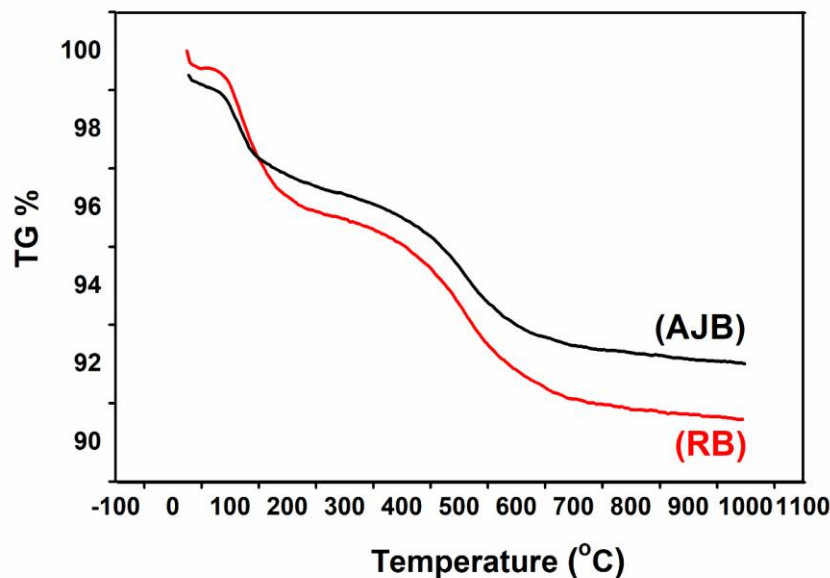


Fig 3: TGA curves of RB and AJB.

BET surface area

The results of BET analysis show that the surface area increases with increasing Na on the surface of bentonite. The surface area increases from 66.2 m²g⁻¹ for RB to 249.6m²g⁻¹ for AJB. The improved surface area indicates the number of active sites increase on the surface of the adsorbent, which improves the enhancement in adsorption efficiency [42].

In studying the adsorption and swelling properties of the clay-water system, onetype of swelling, commonly known as the interlayer or interlamellar swelling, involves the expansion of the crystal lattice itself, as found in montmorillonite [43].It is known that the swelling properties of bentonite depend on the type of exchangeable cations, whether Na⁺ or Ca²⁺. Calcium ions have a higher charge and smaller diameter than sodium ions, and as a result they tend to interact more strongly with the aluminosilicate platelets, thus making them less disposed to swelling. Sodium ions hydrate more readily causes the bentonite to swell more, so any effort to increase the concentration of Na⁺ ions will improve the swelling properties of bentonite [44]. This is perfectly consistent with the obtained XRD result. However, improved swelling of bentonite after activation is expected to yield an increase in pore size and thus an increase in adsorption capacity. Consequently, it improves the removal of heavy metal ions and phenolic compounds.

Characterization of OMWW

The characteristics of the studied crude and treated OMWW are summarized in the following Table:



Table 1: Main characteristics of OMWW sample: untreated and treated with RB and AJB.

Parameters	Untreated OMWW	Literature ranges values	Reference	Treated OMWW with RB	Treated OMWW with AJB	% Removal using RB	% Removal using AJB
pH	4.63	4.9 – 6.50	[⁴⁵]	5.74	6.66	----	----
Conductivity, ms/cm	19.89	13 – 50	[^{46, 47}]	19.4	17.2	----	----
Sodium (Na ⁺), mg L ⁻¹	297.9	200 – 570	[^{48, 49}]	186.4	119.4	37.4	59.9
Potassium (K ⁺), mg L ⁻¹	6366.3	639 – 10800	[^{50, 51}]	4075.1	2606.3	35.9	59.1
Total phenolic compounds, GAE/L	1.34	0.26 – 10.7	[^{52, 53}]	0.85	0.44	36.6	67.2
Alkalinity (CaCO ₃), mg L ⁻¹	2000	3150 – 9070	[⁵⁴]	1500	500	25.0	75.0
Total Chlorine, mg L ⁻¹	20	33.3 – 142.7	[⁵⁵]	15	7	25.0	65.0
Phosphate (PO ₄ ³⁻), mg L ⁻¹	4120	31.8 – 1820	[⁵⁶]	460	230	88.8	94.4
Nitrate (NO ₃ ⁻ -N), mg L ⁻¹	360	350 – 390	[⁵⁷]	230	120	36.1	66.7
COD, mg L ⁻¹	12000	1900 – 220000	[^{58, 59}]	7030	1182	41.4	90.2
DO, mg L ⁻¹	600	n.d.	----	297	281	50.5	53.2
TDS, mg L ⁻¹	34700	5900 – 103200	[⁶⁰]	13140	11899	62.1	65.7
ORP, mv	259800	n.d.	----	73300	58201	71.8	77.6
Salt, mg L ⁻¹	26700	11900 – 32000	[⁶¹]	9930	6321	62.8	77.5

n.d.: not determined. ORP: Oxidation Reduction Potential.

The analysis of the OMWW shows that it is composed mainly of organic compounds and inorganic compounds (mineral salts). Among the different mineral salts present in OMWW, potassium has the highest concentration. Other cations and anions are also found in OMWW at lower concentrations. In addition, the high phenol content of OMWW also contributes to the high soluble COD of OMWW. Total dissolved solids content is also high. Phosphate content is significant. All the above parameters must be taken into consideration in the design of a well-integrated treatment process for OMWW.

It is worth noting here that the parameter values are in good agreement with those reported in the literature. Clearly, using RB for OMWW treatment is essential, due to significant differences between its properties. Furthermore, it is noticed that the percentage removal increases vigorously and continuously throughout the use of AJB adsorbent and this is a good indication that simple activation of bentonite can result in a good result on its adsorption behavior. Therefore, AJB adsorbent provides a valuable solution toward the treatment and recyclability of OMWW.

Adsorption Experiments

Total phenolic compounds removal

Both RB and AJB were tested for the removal of total phenolic compounds and batch experiments were performed, where several parameters were tested, in order to determine the adsorption effectiveness. Different adsorbent dosages (0.1, 0.5 and 1.0 g) were mixed with 10 mL of OMWW with different initial total phenolic compounds concentration (1215.16, 1340.64, 1442.00 and 1563.43 mg/L), at different temperatures (293, 303, 313 and 323K). OMWW and adsorbent were stirred in Erlenmeyer flasks continuously for three hrs. After shaking, samples were filtered using a 0.45 μm micro filter and then analyzed by UV-VIS spectrophotometer at λ=765nm, in order to measure the concentration of total phenolic compounds. Finally, all analytical methods were applied at least in triplicate.

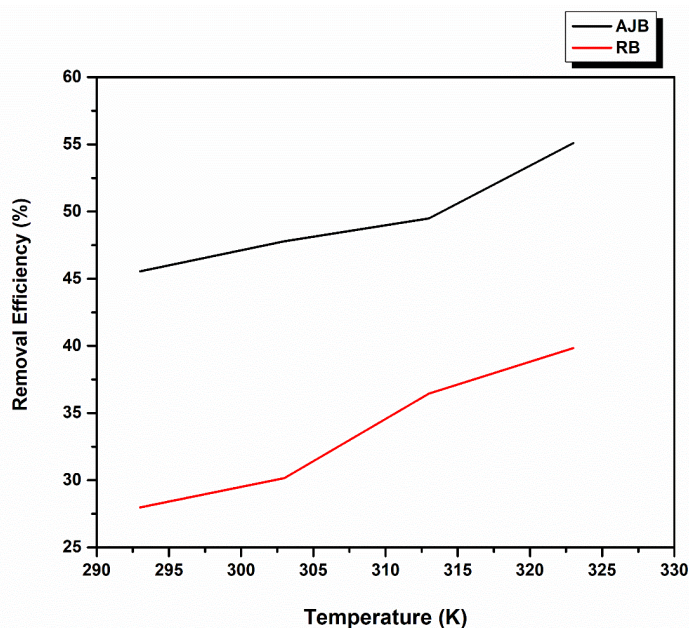


Fig 4: Comparison of the percentage removal of total phenolic compounds by RB and AJB. Mass of adsorbent =1.0 g, initial total phenolic compounds concentration 1340.64 mg/L, 10 mL of OMWW, and contact time =3 hrs.

Adsorption amount of total phenolic compound using AJB is larger than the un-activated one, as shown in Fig. 4. The proposed explanation of the enhanced adsorption involves bentonite having a large specific surface area and pore spaces, and it is based on the diffuse double layer theory, which predicted that double layer thickness decreases with increasing pore-solution concentration [xii]. Therefore, at a given void ratio, the effective porosity of bentonite will increase as the solution concentration increases, which is

beneficial for the adsorption. Moreover, sodium chloride dissociates into Na^+ and Cl^- in aqueous solution. There is a strong electrostatic field around the anions and cations and thus an oriented array of water molecules is formed around these ions. The existence of ions enhances the combining powers between water molecules and phenolic compounds. On the other side, the hydraulic conductivity of the bentonite increases as the void ratio increases. Also, at a given void ratio, the hydraulic conductivity of the bentonite increases, as the ionic strength increases. This trend for increasing hydraulic conductivity probably results from the influence of the permeant on effective porosity (the pore space available for conductive flow), which concludes that increasing the concentration of salts, such as NaCl, leads to an increase in permeability in bentonite due to a decrease in inter-particle repulsion among negative charged plates [lxiii].

As a result of the activation of bentonite by NaCl, adsorption capacity increases towards total phenolic compounds.

Effect of adsorbent dosage on adsorption of total phenolic compounds

The experimental data regarding the effect of adsorbent dosage on the percentage removal of total phenolic compounds by AJB is shown in Fig.5. A series of batch experiments were carried out by contacting different amounts of AJB with 10 mL of OMWW, with a constant initial total phenolic compounds concentration of 1340.64 mg/L. The contact time was made for three hours and at different four temperatures; 293, 303, 313, and 323 K.

The results show that increasing the dosage of AJB resulted in an increase in the percentage removal of total phenolic compounds. However, the adsorption capacity of AJB increases, and this could be due to an increase in the surface area and the availability of more active sites on the surface of AJB [lxiv]. Moreover, the adsorption capacity for AJB is greater than RB at constant temperature and dosage, which indicates that the bentonite is well activated by NaCl. Therefore, in order to reduce the bentonite dosage, it is necessary to modify it into superior Na-Bentonite.

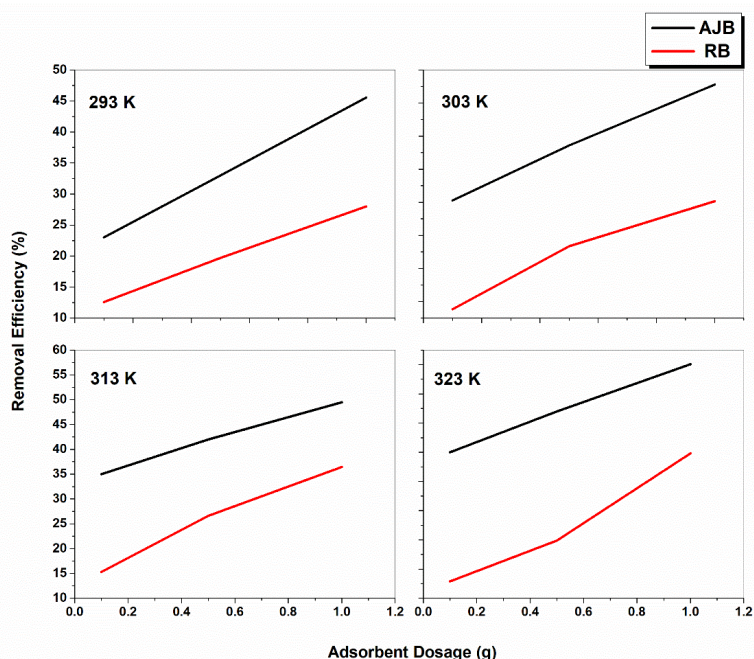


Fig 5: Effect of adsorbent dosage on the percentage removal of total phenolic compounds at different temperatures.

Effect of initial total phenolic compounds concentration

The initial total phenolic compounds concentration is a very important factor to be explored in adsorption studies, as most contaminated OMWW usually present different concentrations of total phenolic compounds. The effect of initial total phenolic compounds concentration on the adsorption capacity and percentage removal is shown in Fig. 6. The operating conditions for the batch experiments were 1.0 g of AJB per 10 mL of OMWW and the contact time was three hours at 303 K.

Firstly, an increase in adsorption capacity with an increase in initial total phenolic compounds concentration was observed. This may be explained by the presence of more total phenolic compounds in the solution available for binding onto the active sites of the AJB. Consequently, the adsorption reached a saturation value. Indeed, the initial total phenolic compounds concentration provides an important driving force to overcome all mass transfer resistance. Hence a higher initial concentration of total phenolic compounds tends to enhance the adsorption capacity. A similar phenomenon was observed for the adsorption of phenol onto organ obentonite. Meanwhile, the percentage removal decreased gradually with an increase in the initial total phenolic compounds concentration. This decrease is due to the fact that all adsorbents have a limited number of active sites, and at higher concentrations the active sites become saturated.

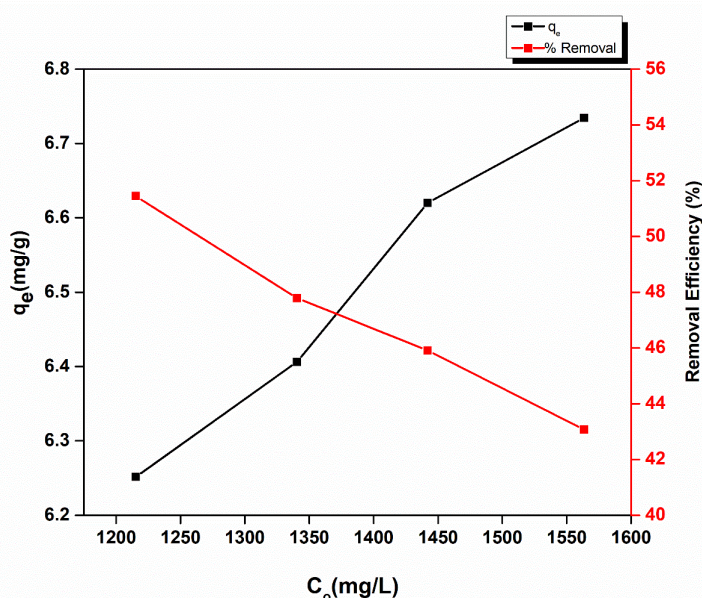


Fig 6: Effect of initial total phenolic compounds concentration on the adsorption capacity and the percentage removal of total phenolic compounds.

Adsorption Isotherms

The adsorption isotherms for total phenolic compounds removal by AJB were investigated using different initial concentrations at adsorbent mass of 1.0 g at 293, 303, 313 and 323 K and for a period of three hours. Later, the data obtained were fitted to the Langmuir and Freundlich isotherms.

The Langmuir isotherm assumed that the monolayer adsorption of adsorbate onto a homogeneous adsorbent surface takes place with a single coating layer on this surface. Moreover, there is no lateral interaction between the adsorbed molecules. The linear form of the Langmuir isotherm model can be expressed as:

$$\frac{C_e}{q_e} = \frac{1}{K_L q_m} + \frac{C_e}{q_m} \quad (4)$$

where q_e is equilibrium adsorption capacity(mg/g); C_e is the equilibrium concentration of total phenolic compounds(mg/L); q_m is a maximum adsorption capacity (mg/g); and K_L is the adsorption equilibrium constant(L/mg).

The linear form of the Langmuir isotherm is shown in Fig. 7. The correlation coefficients, R^2 are > 0.99 at all temperatures, indicate that the adsorption was a good fit to this model.

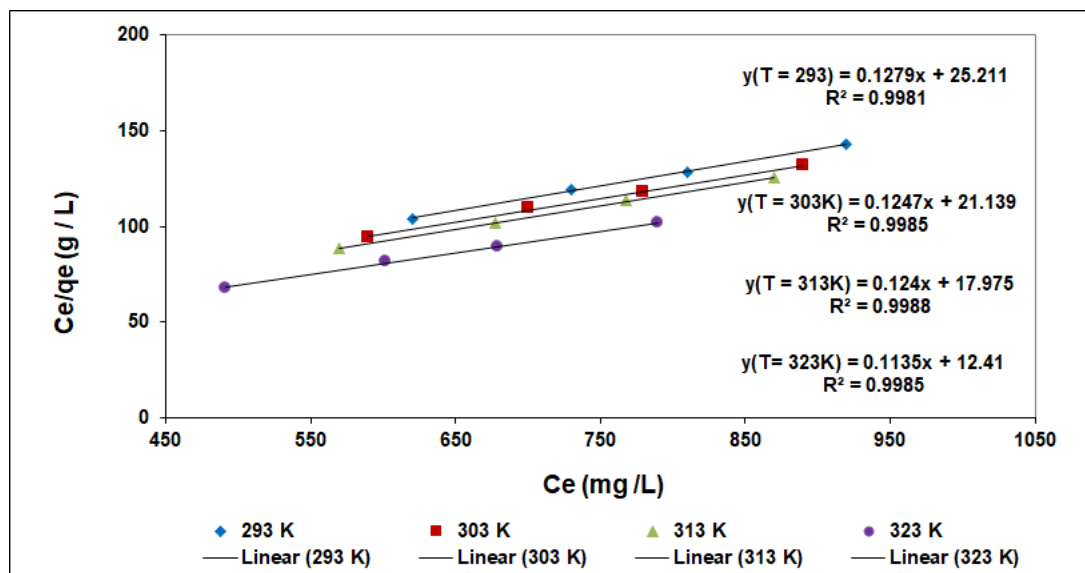


Fig 7: Langmuir plot for the adsorption of total phenolic compounds onto AJB. Adsorbent dosage: 1.0 g, 10mL of OMWW, pH =6, contact time =3 hrs.

The maximum adsorption q_m for total phenolic compounds onto AJB equals to 8.81 mg/g. The adsorption process can be evaluated to see whether it is favorable by the use of a Langmuir dimension less separation factor R_L defined as:

$$R_L = \frac{1}{1 + K_L C_o} \quad (5)$$

where C_o (mg/L) is the initial metal ion concentration in solution. If the value of R_L is less than 1.0, the adsorption is considered to be favorable, but it is unfavorable if R_L is greater than 1.0. The calculated R_L values at different concentrations fall within the range of 0.098–0.122 (Table 2), thus indicating a favorable adsorption process.

Table 2: Calculated values of separation factor R_L for the adsorption of total phenolic compounds onto AJB at 303 K.

C_o	1215.16	1340.64	1442.00	1563.43
R_L	0.1224	0.1123	0.1052	0.0978

The Freundlich isotherm is based on multilayer adsorption on heterogeneous surface [lxv]. The linear form of Freundlich can be represented as:

$$\log q_e = \log K_F + \frac{1}{n} \log C_e \quad (6)$$

where K_F and n are the Freundlich adsorption constants showing the adsorption capacity (mg/g) and intensity, respectively, which can be determined by the linear plot of $\log q_e$ versus $\log C_e$.

The adsorption Freundlich isotherm obtained for total phenolic compounds onto AJB are shown in Fig.8, and the isotherm parameters for both models are presented in Table 3.

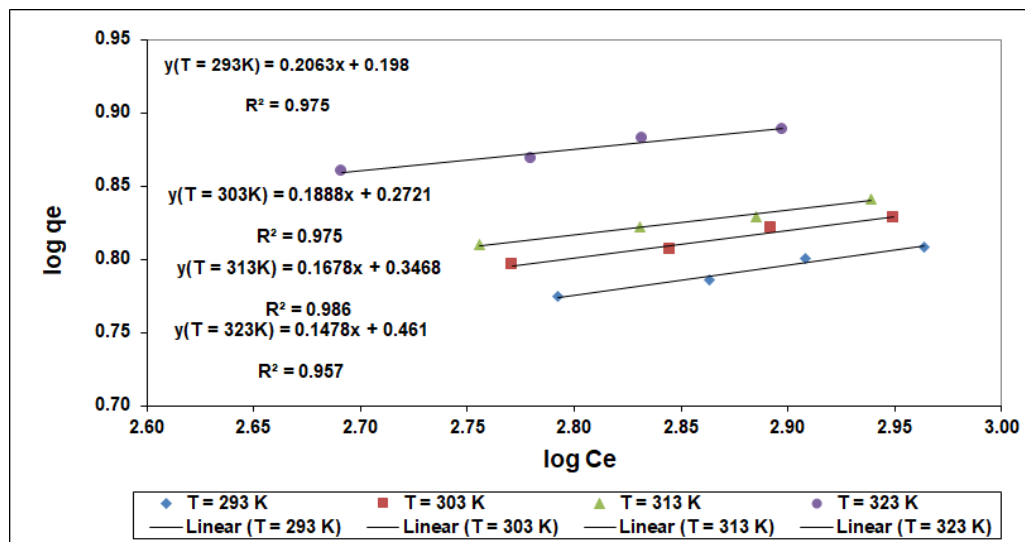


Fig 8: Freundlich plot for the adsorption of total phenolic compounds onto AJB. Adsorbent dosage: 1.0 g, 10 mL of OMWW, pH =6, contact time =3 hrs.

Table 3: Langmuir and Freundlich Isotherm parameters for the adsorption of total phenolic compounds onto AJB.

T (K)	Langmuir Isotherm			Freundlich Isotherm		
	q_m	K_L	R^2	n	K_F	R^2
293	7.8168	0.0051	0.9981	4.8481	1.5774	0.9754
303	8.0201	0.0059	0.9985	5.2958	1.8710	0.9753
313	8.0640	0.0069	0.9988	5.9604	2.2222	0.9860
323	8.8128	0.0091	0.9985	6.7648	2.8905	0.9576

The obtained values of n exhibited intense change at higher temperatures. All n values were greater than one, indicating a favorable adsorption of total phenolic compounds [16]. Also, the high correlation coefficient values (R^2) of the Langmuir and Freundlich model indicate that the experimental data are well fitted by both models.

Thermodynamic Studies

Effect of temperature on adsorption of total phenolic compounds

In order to determine the effect of temperature on the adsorption of total phenolic compounds onto AJB, experiments were run with four different values: 293, 303, 313 and 323 K. From the curves of Fig. 9, we can notice that the percentage of efficiency removal of total phenolic compounds increases with temperature, which indicates that the adsorption process is endothermic. This may be due to increasing the mobility of the total phenolic compounds, thus gaining more kinetic energy to diffuse from the bulk phase to the solid phase, with an increase in solution temperature. Furthermore, there is an increase in the number of surface active sites for the adsorption with increasing temperature, as a result of the dissociation of some of the surface components onto AJB [17, 18]. On the other hand, K_L values are directly proportional to the temperature, as shown in Fig.9. K_L is the Langmuir equilibrium constant related to the affinity of binding sites and energy of

sorption, equation (4). Again, the total phenolic compounds have a good affinity to the AJB surface and increase gradually with increasing temperature. Similarly, at constant initial total phenolic compounds concentration (1340.64mg/L) and fixed dosage of both adsorbents (1g), as clearly observed in Fig. 9, the percentage removal of total phenolic compounds using RB adsorbent increases with increasing temperature.

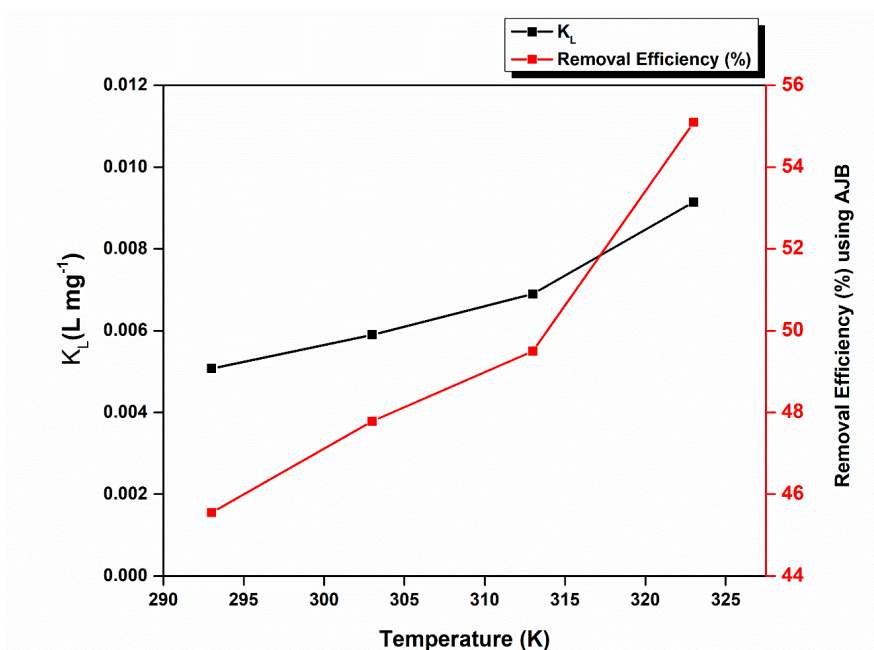


Fig 9: Effect of solution temperature on the percentage removal of total phenolic compounds and the Langmuir equilibrium constant K_L using AJB.

Temperature has an obvious effect on sodium modification of the bentonite, and Na^+ in the diffusion layer present has a trend of moving to bentonite surfaces. Migration of Na^+ is increased, which increases the content of Na^+ on the bentonite surface. Therefore, the reaction velocity between Na^+ and Ca^{2+} is growing.

In order to evaluate the feasibility of the adsorption process, thermodynamic parameters, where ΔG° is the Gibbs free energy (kJ/mol), ΔH° is the standard enthalpy (J/mol) and ΔS° is the standard entropy (J/mol K), were calculated from the curve relating the distribution coefficient (K) as a function of temperature, using the following equations:

$$\Delta G^\circ = -RT \ln K \tag{7}$$

$$\ln K = \frac{\Delta S^\circ}{R} - \frac{\Delta H^\circ}{RT} \tag{8}$$

Where R is the gas constant (8.3145 J.mol⁻¹.K⁻¹), T is the temperature in Kelvin. The values of ΔH° , ΔS° were determined from the slope and intercept values of the straight line of plotting $\ln K$ versus $1/T$, respectively. According to data presented in Table 4, the spontaneity of the adsorption process is established by a decrease in ΔG° values, in addition to spontaneity increases as the temperature of solution increases, which means that, as the adsorption process becomes more favorable, the negative values of ΔG° indicate that the adsorption of the total phenolic compounds is spontaneous and favorable [ix]. The positive value of ΔH° shows that the adsorption process is endothermic in nature. This is in accordance with increasing adsorption equilibrium with increasing temperature. The positive value of ΔS° reflects an increase in the randomness at the interface between AJB and the Phenolic solution during the adsorption process. This suggests that some structural changes occur on the adsorbent, in addition to the adsorbate, due to the exchange of the phenolic compounds with more mobile ions present on the AJB, which would cause an increase in the entropy during the adsorption process.

Table 4: Thermodynamic parameters of adsorption of total phenolic compounds onto AJB

T (K)	ΔH°	ΔS°	ΔG°
293			26.22
303	559.47	1.81	13.90
313			-5.22
323			-28.21

Moreover, the ΔH° value was $559.47 \gg 60$ kJ/mol [lxx], thus indicating the adsorption of total phenolic compounds onto AJB involved chemical adsorption. Therefore, the process is irreversible.

Heavy metal ions removal

It is known that the main mineral in bentonite is montmorillonite, which has a large specific surface, in addition to a large net negative charge, which results in adsorption of a large number of hydrated cations.

Column adsorption technique was utilized for removing the metal ions from the OMWW. Figs. 10, 11 and 12 show the percentage uptake of heavy metal ions by RB and AJB. In contrast with RB, cation exchange capacity appears to be more reliable, where the exchangeable Na^+ ions of the AJB were high, and consequently the adsorption capabilities of heavy metals are increased. Ashmawy et al. (2005) stated the same results [lxxi].

In general, using Na-Bentonite is better than that using Ca-Bentonite, if the dosage is equal [lxxii].

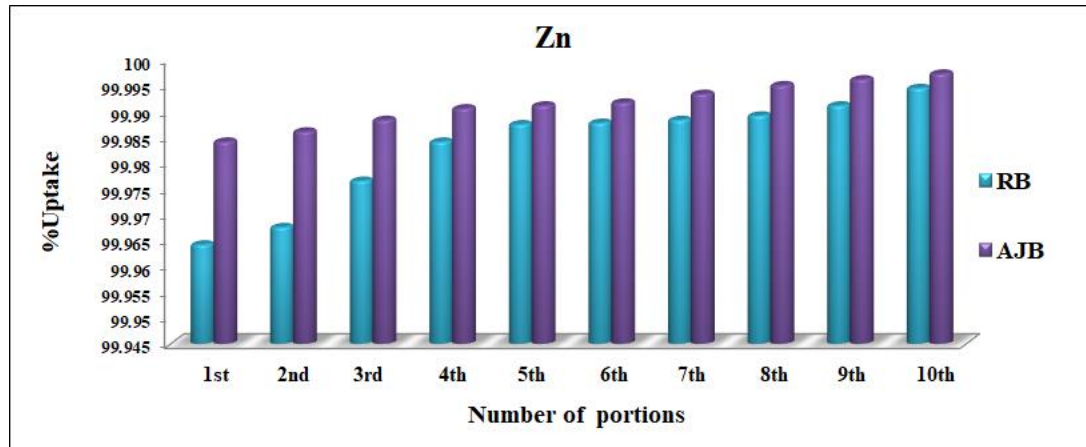


Fig 10: Percentage uptake of Zn(II) by RB and AJB using column technique.

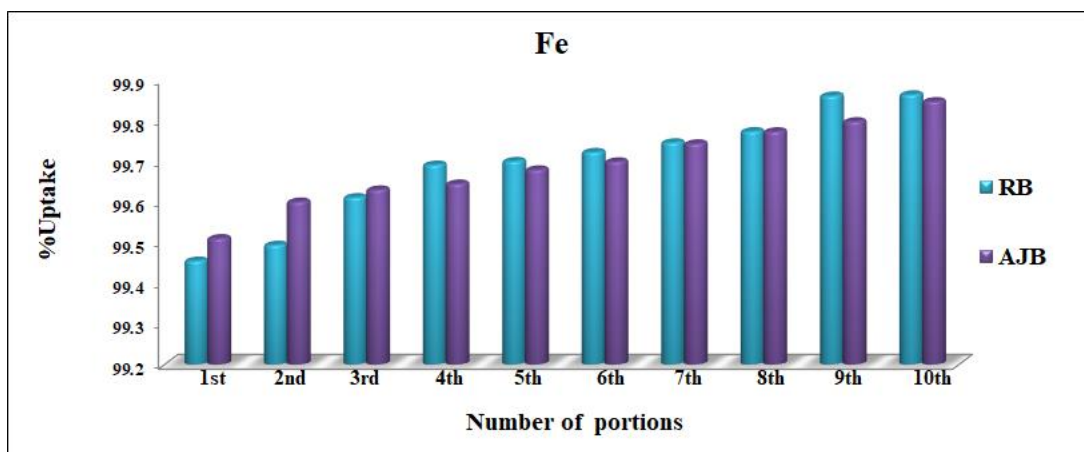


Fig 11: Percentage uptake of Fe(II) by RB and AJB using column technique.

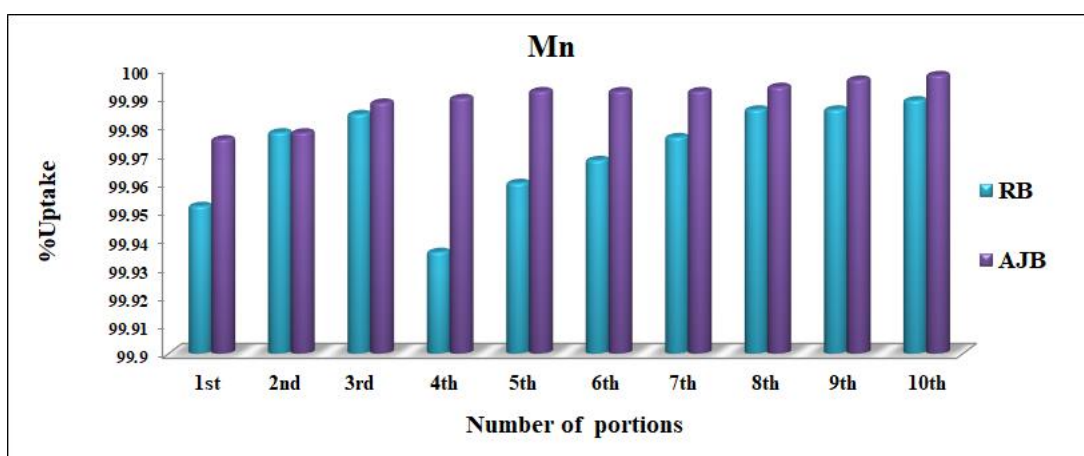


Fig 12: Percentage uptake of Mn(II) by RB and AJB using column technique.

Moreover, the effect of contact time was studied. Fig. 13 shows the effect of agitation time with constant initial metal ion concentration (3573, 2025 and 1242mg/L for Zn, Fe and Mn ions, respectively) on the adsorption capacity of AJB. It was observed that the amount of adsorbed metal ion (q) increases with an increase in contact time at all initial metal ion concentrations. Furthermore, for the first 10 min, the percentage removal was rapid and exceeded 99.5%. It then proceeds at a slower adsorption rate and finally it reaches saturation at 60, 80 and 48 min for Zn, Fe and Mn ions, respectively. Also, the plots show that the initial metal ion concentration has no effect on the required time for equilibrium. Thus, the higher adsorption rate at the initial period may be due to the increased number of unoccupied sites available at the initial stage, which is due to the existing increase in the concentration gradients between adsorbate in solution and adsorbate on the adsorbent surface. As time proceeds, the metal ion concentration is reduced, due to the accumulation of metal ions in the available sites, leading to a decrease in the adsorption rate at later stages.

Clearly, AJB can completely remove all heavy metal ions from OMWW, regardless of their initial concentrations.

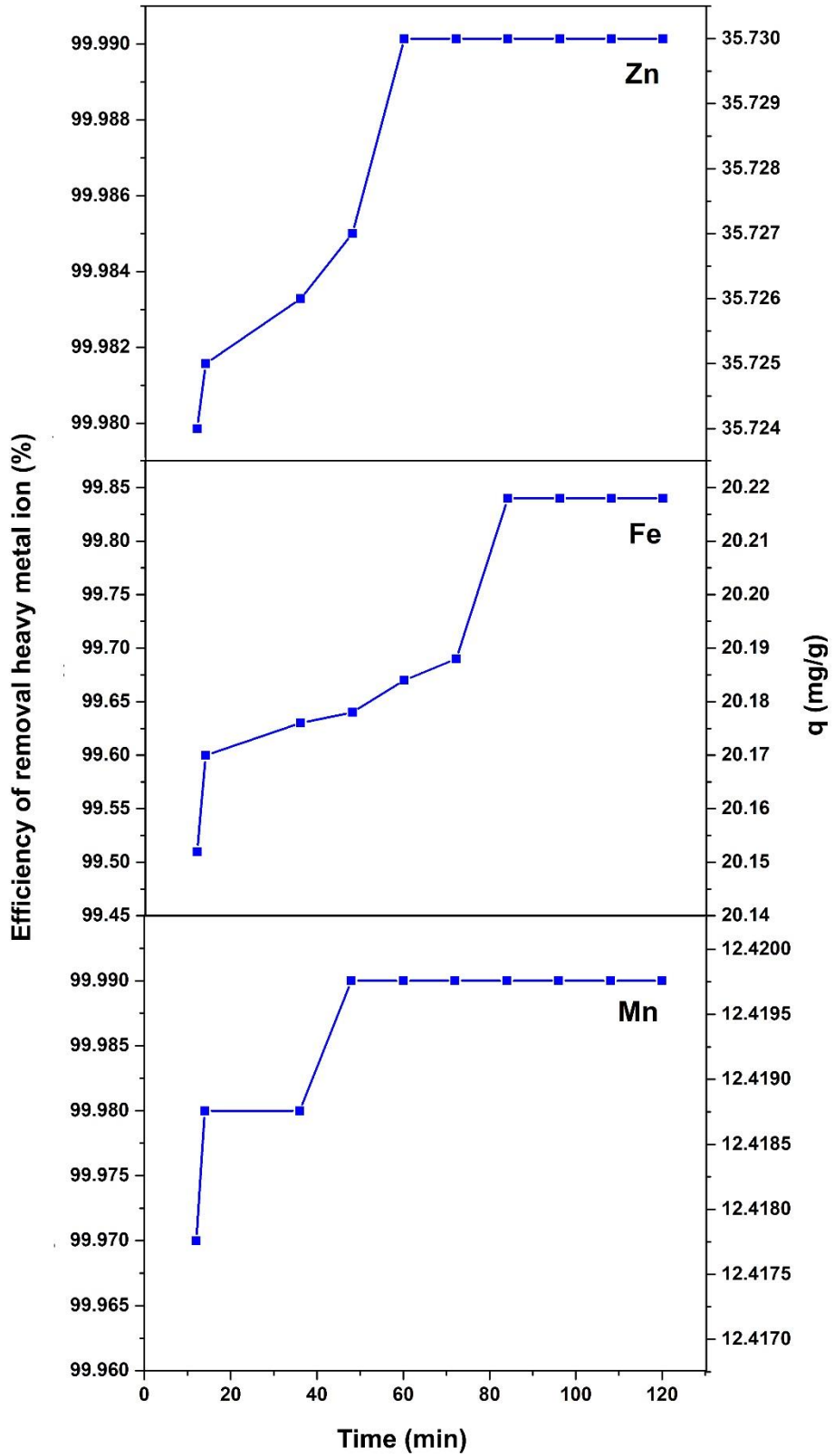


Fig 13: The effect of contact time on the adsorption capacity and percentage removal of Zn, Fe and Mn ions using AJB.

According to the results obtained from this work, by using effectively prepared AJB adsorbent, it is favorable in terms of both economic and environmental features and it could improve adsorption for the removal of hazardous materials, such as Phenolic compounds and heavy metal ions from industrial effluents such as OMWW.

CONCLUSION

The management of produced OMWW is a particularly unsolved problem, especially in Jordan, due to their high content of phenolic compounds, their physicochemical composition, and the implicit toxic merits. More effective, simple, low cost and environmental friendly methods are needed mainly in developing countries.

The present study presents a successful method for activation Jordanian bentonite using sodium chloride. FTIR, XRD and TGA studies have approved this method, in addition to the increase in its surface area. Subsequently, the AJB has been examined as an adsorbent for OMWW treatment. The physicochemical analysis appears to show a good performance for AJB, which can help to reduce environmental damage, prevent groundwater contamination and provide an alternative approach for olive mills, in regards to safe utilization of OMWW. Moreover, AJB shows a great potential for the removal of heavy metal ions and phenolic compounds pollutants. Results show percentage uptakes exceeding 99.99 % for Zn, Fe and Mn ions: and the percentage removal for phenolic compounds can be considered as satisfactory. Adsorption efficiency is strongly affected by parameters, such as adsorbent dosage, initial total phenolic compounds concentration, and the temperature of the solution. On the other hand, its equilibrium adsorption was well fitted to the Langmuir and Freundlich models. Thermodynamics studies have confirmed that the adsorption process was spontaneous and endothermic in nature.

Notably, the AJB shows a substantially higher adsorption capacity compared to the RB. This study provides a feasible method for utilizing activated bentonite for application in waste water treatment.

ACKNOWLEDGMENTS

The author is grateful for the Support to Research and Technological Development & Innovation Initiatives and Strategies in Jordan (SRTD II) and the European Union Funded Project, Budget line BGUE-2011-19.080101-CI-DEVCO, Reference: SRTD/2014/GRT/AR/2321, for having funded the project, in addition to Jerash University.

Conflict of interest: The author declares that there is no conflict of interests regarding the publication of this manuscript.

REFERENCES

-
- [1] M. Aggoun, R. Arhab, A. Cornu, J. Portelli, M. Barkat, B. Graulet, Olive mill wastewater microconstituents composition according to olive variety and extraction process, *Food Chemistry* 209 (2016) 72-80.
 - [2] L. C. Davies, A. M. Vilhena, J. M. Novais, S. Martins-Dias, Olive mill wastewater characteristics: modelling and statistical analysis, *Grasas y Aceites* 55 (3) (2004) 233-241.
 - [3] M. Jeguirim, P. Dutournié, A. A. Zorpas, L. Limousy, Olive Mill Wastewater: From a Pollutant to Green Fuels, Agricultural Water Source and Bio-Fertilizer—Part 1. The Drying Kinetics, *Energies* 10 (2017) 1423-1439.
 - [4] S. Ibrahim, L. Yael, R. Michael, M. Shlomit, Land spreading of olive mill wastewater: Effects on soil microbial activity and potential phytotoxicity, *Chemosphere* 66 (1) (2007) 75-83.

-
- [5] D. Dimitrios, N. Ioanna, K. Michalis; D. Stefanos, Olive oil mill wastewater toxicity in the marine environment: Alterations of stress indices in tissues of mussel *Mytilus galloprovincialis*, *Aquatic Toxicology* 101(2) (2011) 358-366.
- [6] S. Kulkarni, J. Kaware, Regeneration and Recovery in Adsorption- a Review, *International Journal of Innovative Science, Engineering & Technology* 1(8) (2014) 61–64.
- [7] A. A. Adeyemo, I. O. Adeoye, O. S. Bello, Adsorption of dyes using different types of clay: a review, *Appl Water Sci.* 7 (2017) 543–568.
- [8] S. Abd Hamid, M. Shahadat, S. Ismail, Development of cost effective bentonite adsorbent coating for the removal of organic pollutant, *Applied Clay Science* 149 (2017) 79-86.
- [9] Z. Huang, Y. Li, W. Chen, J. Shi, N. Zhang, X. Wang, Z. Li, L. Gao, Y. Zhang, Modified bentonite adsorption of organic pollutants of dye wastewater, *Materials Chemistry and Physics* 202 (2017) 266-276.
- [10] J. Ma, J. Qi, C. Yao, B. Cui, T. Zhang, D. Li, A novel bentonite-based adsorbent for anionic pollutant removal from water, *Chemical Engineering Journal* 200–202 (2012) 97-103.
- [11] N. Belhouchat, H. Zaghoulane-Boudiaf, C. Viseras, Removal of anionic and cationic dyes from aqueous solution with activated organo-bentonite/sodium alginate encapsulated beads, *Applied Clay Science* 135 (2017) 9-15.
- [12] J. G. Meneguín, M. P. Moisés, T. Karchiyappan, S. Faria, M. L. Gimenes, M. A. Barros, S. Venkatachalam, Preparation and characterization of calcium treated bentonite clay and its application for the removal of lead and cadmium ions: Adsorption and thermodynamic modeling, *Process Safety and Environmental Protection* 111 (2017) 244-252.
- [13] D. Bouazza, H. Miloudi, M. Adjdir, A. Tayeb, A. Boos, Competitive adsorption of Cu (II) and Zn (II) on impregnate raw Algerian bentonite and efficiency of extraction, *Applied Clay Science* 151 (2018) 118-123.
- [14] Y. Chen, J. Peng, H. Xiao, H. Peng, L. Bu, Z. Pan, Y. He, F. Chen, X. Wang, S. Li, Adsorption behavior of hydrotalcite-like modified bentonite for Pb²⁺, Cu²⁺ and methyl orange removal from water, *Applied Surface Science* 420 (2017) 773-781.
- [15] H. Babaki, A. Salem, A. Jafarizad, Kinetic model for the isothermal activation of bentonite by sulfuric acid, *Materials Chemistry & Physics* 108 (2/3) (2008) 263-268.
- [16] W. Bekele, G. Faye, N. Fernandez, Removal of nitrate ion from aqueous solution by modified ethiopian bentonite clay, *International Journal of Research in Pharmacy and Chemistry* 4(1) (2014) 192-201.
- [17] S. Hashemian, B. Sadeghi, F. Mozafari, H. Salehifar, K. Salari, Adsorption of Disperse of Yellow 42 onto Bentonite and Organo-Modified Bentonite by Tetra Butyl Ammonium Iodide (B-TBAI), *Polish Journal of Environmental Studies* 22 (5) (2013) 1363-1370.
- [18] N. Belhouchat, H. Zaghoulane-Boudiaf, C. Viseras, Removal of anionic and cationic dyes from aqueous solution with activated organo-bentonite/sodium alginate encapsulated beads, *Applied Clay Science* 135 (2017) 9-15.
- [19] Z. Huilin, L. Xiaoyu, Y. Chao, N. Chungu, W. Jide; S. Xintai, Nano γ -Fe₂O₃/bentonite magnetic composites: Synthesis, characterization and application as adsorbents, *Journal of Alloys & Compounds Part A* 688 (2016) 1019-1027.
- [20] K. Hu, D. Zhao, J. Liu, Synthesis of nano-MoS₂/bentonite composite and its application for removal of organic dye, *Transactions of Nonferrous Metals Society of China* 22(10) (2012) 2484-2490.

- [21] S. Pandey, A comprehensive review on recent developments in bentonite-based materials used as adsorbents for wastewater treatment, *Journal of Molecular Liquids* 241 (2017) 1091-1113.
- [22] J. Hua, Adsorption of low-concentration arsenic from water by co-modified bentonite with manganese oxides and poly(dimethyldiallylammonium chloride), *Journal of Environmental Chemical Engineering* 6 (1) (2018) 156-168.
- [23] T. Schütz, S. Dolinská, P. Hudec, A. Mockovčíaková, I. Znamenáčková, Cadmium adsorption on manganese modified bentonite and bentonite–quartz sand blend, *International Journal of Mineral Processing* 150 (2016) 32-38.
- [24] M. I. Magzoub, M. S. Nasser, I. A. Hussein, A. Benamor, S. A. Onaizi, A. S. Sultan, M. A. Mahmoud, Effects of sodium carbonate addition, heat and agitation on swelling and rheological behavior of Ca-bentonite colloidal dispersions, *Applied Clay Science* 147 (2017) 176-183.
- [25] C. A. Santi, S. Cortes, L. P. D'Acqui, E. Sparvoli, B. Pushparaj, Reduction of organic pollutants in Olive Mill Wastewater by using different mineral substrates as adsorbents, *Bioresource Technology* 99 (6) (2008) 1945-1951.
- [26] M. A. Mahasneh, K. S. Shakhathreh, Evaluation of Jordanian Bentonite Performance for Drilling Fluid Applications, *Contemporary Engineering Sciences* 5(3) (2012) 149–170.
- [27] I. Hamadneh, R. abu -Zurayk, b. abu -Irmaileh, A. bozeyya, A. Al – Dujaili, adsorption of pb(II) on raw and organically modified jordanian bentonite, *clay minerals* 50 (2015) 485–496.
- [28] F. I. Khalili, N. H. Salameh, M. M. Shaybe, Sorption of Uranium(VI) and Thorium(IV) by Jordanian Bentonite, *Journal of Chemistry* 2013 (2013) 1-13.
- [29] R. A. Al Dwairi, A. E. Al-Rawajfeh, Removal of cobalt and nickel from wastewater by using Jordan low-cost zeolite and bentonite, *Journal of the University of Chemical Technology and Metallurgy* 47 (1) (2012) 69-76.
- [30] I. Leouifoudi, A. Ziyad, A. Amechrouq, M. Oukerrou, H. Mouse, M. Mbarki, Identification and characterisation of phenolic compounds extracted from Moroccan olive mill wastewater, *Food Sci. Technol, (Campinas)* 34(2) (2014) 249–257.
- [31] J., Madejova, J., Kec'ke's, H. Pa'lkova, P. Komadel, Identification of components in smectite/kaolinite mixtures, *Clay Minerals* 37(2) (2002) 377–388.
- [32] W. K. Mekhamer, Energy storage through adsorption and desorption of water vapour in raw Saudi bentonite, *Arabian Journal of Chemistry* 9 (2016) S264–S268.
- [33] L. Zhirong, M. Azhar Uddin, S. Zhanxue, [FT-IR and XRD analysis of natural Na-bentonite and Cu\(II\)-loaded Na-bentonite.](#) *Spectrochimica Acta Part A: Molecular and Biomolecular Spectroscopy* 79(5) (2011) 101-1016.
- [34] A. Tabak, B. Afsin, B. Caglar, E. Koksals, Characterization and pillaring of a Turkish bentonite (Resadiye), *Journal of Colloid and Interface Science* 313(1), (2007) 5–11.
- [35] R. Ajemba, Structural alteration of bentonite from nkaliki by acid treatment: studies of the kinetics and properties of the modified samples. *International Journal of Advances in Engineering & Technology* 7(1) (2014) 379-392.
- [36] D. M. Manohar, B. F. Noeline, T. S. Anirudhan, Adsorption performance of Al-pillared bentonite clay for the removal of cobalt(II) from aqueous phase, *Applied Clay Science* 31(3-4) (2006) 194–206.

- [37] M. Naswir, S. Arita, Marsi., Salni , Characterization of bentonite by XRD and SEM-EDS and use to increase pH and color removal, Fe and organic substances in peat water, *Journal of Clean Energy Technologies* 1(4) (2013) 313-317.
- [38] G. Batdemberel, T. Battumur, Ts. Enkhtuya, G. Tsermaa, Sh. Chadraabal, Synthesis of ZnO Nanoparticles by Mechanochemical Processing, Conference: Proceedings of the 4th International Conference on X-ray Analysis, Volume-I, pages 47-48. Ulaanbaatar, Mongolia, 8-12 June (2015) DDC 616.07572, ISBN: 978-99975-55-92-8.
- [39] K. Margeta, N. Z. Logar, M. Šiljeg, A. Farkas, "Water Treatment", Chapter 5 (Natural Zeolites in Water Treatment – How Effective is Their Use) book edited by Walid Elshorbagy and Rezaul Kabir Chowdhury, ISBN 978-953-51-0928-0, 2013 under CC BY 3.0 license. Pages 81-111.
- [40] Y. Huang, Y. Zhang, G. Han, T. Jiang, G. Li, Y. Yang, B. Xu, Y. Guo, Sodium-modification of Ca-based bentonite via semidry process, [Journal of Central South University of Technology](#) 17(6) (2010) 1201-1206.
- [41] R. A. Sheikh, The synthesis of cementitious compounds in molten salts, phd thesis, Department of Chemical Engineering University College London, 2016.
- [42] K. G. Akpomie, F. A. Dawodu, K. O. Adebawale, Mechanism on the sorption of heavy metals from binary-solution by a low cost montmorillonite and its desorption potential, *Alexandria Engineering Journal* 54 (2015) 757–767.
- [43] M. E. Elmashad, Effect of chemical additives on consistency, infiltration rate and swelling characteristics of bentonite, *Water Science* 31 (2017) 177–188.
- [44] T. Schanz, S. Tripathy, Swelling pressure of a divalent-rich bentonite: Diffuse double-layer theory revisited, *Water Resources Research* 45(2009) 1-9.
- [45] P. Galiatsatou, M. Metaxas, D. Arapoglou, V. Kasselouri-Rigopoulou, Treatment of olive mill waste water with activated carbons from agricultural by-products, *Waste Management* 22 (2002) 803-812.
- [46] A. Sassi, A. Boularbah, A. Jaouad, G. Walker, A. Boussaid, A comparison of olive oil mill wastewaters (OMW) from three different processes in Morocco, *Process Biochemistry* 41 (1) (2006) 74-78.
- [47] M. Di Serio, B. Lanza, M. Mucciarella, F. Russi, E. Iannucci, P. Marfisi, A. Madeo, Effects of olive mill wastewater spreading on the physico-chemical and microbiological characteristics of soil, *International Biodeterioration and Biodegradation* 62 (2008) 403-407.
- [48] C. Piperidou, C. Chaidou, D. Stalikas, K. Soulti, G. Pilidis, C. Balis, Bioremediation of olive oil mill wastewater: chemical alterations induced by Azotobacter vinelandii, *Journal of Agricultural and Food Chemistry* 48 (2000) 1941-1948.
- [49] E. Eroglu, I. Eroglu, U. Gündüz, M. Yücel, Effect of clay pretreatment on photofermentative hydrogen production from olive mill wastewater, *Bioresource Technology* 99 (2008) 6799-6808.
- [50] F. Hanafi, N. Sadif, O. Assobhei, M. Mountadar, "Traitement des Margines par électrocoagulation Avec des électrodes Plates en Aluminium," *Journal of Water Science* 22 (4) (2009) 473-485.
- [51] E. Moreno, J. Pérez, A. Ramos-Cormenzana, J. Martínez, Antimicrobial effect of waste water from olive oil extraction plants selecting soil bacteria after incubation with diluted waste, *Microbios* 51 (1987) 169-174.
- [52] A. Vlyssides, M. Loizides, P. Karlis, Integrated strategic approach for reusing olive oil extraction by-products, *Journal of Cleaner Production* 12 (6) (2004) 603-611.

-
- [53] F. Hanafi, N. Sadif, O. Assobhei, M. Mountadar, "Traitement des Margines par électrocoagulation Avec des électrodes Plates en Aluminium," *Journal of Water Science* 22 (4) (2009) 473-485.
- [54] M. Mouncif, S. Tamoh, M. Faid, A. Achkari-Begdouri, A study of chemical and microbiological characteristics of olive mill waste water in Morocco, *Grasas y Aceites* 44 (1993) 335-338.
- [55] D. Bouknana, B. Hammouti, R. Salghi, S. Jodeh, A. Zarrouk, I. Warad, A. Aouniti, M. Sbaa, Physicochemical characterization of olive oil mill wastewaters in the eastern region of morocco, *J. Mater. Environ. Sci.* 5 (4) (2014) 1039-1058.
- [56] A. Aly, Y. Hasan, A. Al-Farraj, Olive mill wastewater treatment using a simple zeolite-based low-cost method, *Journal of Environmental Management* 145 (2014) 341-348.
- [57] M. Panizza, G. Cerisola, [Olive mill wastewater treatment by anodic oxidation with parallel plate electrodes](#), *Water Research* 40 (2006) 1179-1184.
- [58] J. Alba, (1994). Nuevas tecnologías para la obtención del aceite de oliva. *Fruticultura Profesional (Suplemento)* 62, 85-95.
- [59] P. Passarinho, Olive Mill Wastewater detoxification. PhD Thesis, Instituto Superior Técnico, Universidade Técnica de Lisboa, Portugal. (2002).
- [60] M. Hamdi, Thermoacidic precipitation of darkly coloured polyphenols of olive mill wastewaters, *Environmental Technology* 14 (1993)495-500.
- [61] M. Mouncif, S. Tamoh, M. Faid, A. Achkari-Begdouri, A study of chemical and microbiological characteristics of olive mill waste water in Morocco, *Grasas y Aceites* 44 (1993) 335-338.
- [62] R. Kant, M. Singh, Generalization of Linearized Gouy-Chapman-Stern Model of Electric Double Layer for Nanostructured and Porous Electrodes: Deterministic and Stochastic Morphology, *Physical Review E* 88(5) (2013) 1- 36.
- [63] M. C. Setz, K. Tian, C. H. Benson, S. L. Bradshaw, Effect of ammonium on the hydraulic conductivity of geosynthetic clay liners, *Geotextiles and Geomembranes* 45 (2017) 665-673.
- [64] J. Acharya, JN. Sahu, CR. Mohanty, BC. Meikap, Removal of lead (II) from wastewater by activated carbon developed from Tamarind wood by zinc chloride activation, *J Chem Eng* 2009 (149) (2009) 249–262.
- [65] H. K. Boparai, M. Joseph, D. M. O'Carroll, Kinetics and thermodynamics of cadmium ion removal by adsorption onto nano zerovalent iron particles, *Journal of Hazardous Materials* 186 (2011) 458–465.
- [66] A. A. Inyinbor, F. A. Adekola, G. A. Olatunji, Kinetics, isotherms and thermodynamic modeling of liquid phase adsorption of Rhodamine B dye onto *Raphia hookerie* fruit epicarp, *Water Resources and Industry* 15 (2016)14–27.
- [67] D. Ghahremani, I. Mobasherpour, S. Mirhosseini, Sorption thermodynamic and kinetic studies of Lead removal from aqueous solutions by nano Tricalcium phosphate, *Bulletin de la Société Royale des sciences de Liège* 86 (2017) 96 – 112.
- [68] K.G. Bhattacharyya, S.S. Gupta, Kaolinite, montmorillonite and their modified derivatives as adsorbents for removal of Cu(II) from aqueous solution, *Sep. Purif. Technol.* 50 (2006) 388–397.

-
- [69] N. S. A. Mubarak, A. H. Jawad, W. I. Nawawi, Equilibrium, kinetic and thermodynamic studies of Reactive Red 120 dye adsorption by chitosan beads from aqueous solution, *Energy, Ecology and Environment* 2(1) (2017) 85-93.
- [70] J. Fu, Y. Li, C. Ye, C. Lin, Study on the adsorption kinetics and thermodynamics of DMF on macroporous adsorbents, *Acta Scientiae Circumstantiae*, 32(3) (2012) 639-644.
- [71] A. K. Ashmawy, N. Muhammad, D. Elhajji, Advection, diffusion, and sorption characteristics of inorganic chemicals in GCL bentonite. In *Geo-Frontiers 2005: Waste Containment and Remediation* (Geotechnical Special Publication 142), Rathje, E. M., Editor, American Society of Civil Engineers, Reston, VA, USA, (2005) 3249-3258.
- [72] S. Ding, Y. Sun, C. Yang, B. Xu, Removal of copper from aqueous solutions by bentonites and the factors affecting it, [Mining Science and Technology \(China\)](#) 19(4) (2009) 489-492.